PETROLEUM SCIENCE AND TECHNOLOGY, 19(1&2), 143–156 (2001)

NUMERICAL SIMULATION OF WAX DEPOSITION IN OIL PIPELINE SYSTEMS

E. Ramírez-Jaramillo,[1] C. Lira-Galeana,[1] and O. Manero[2,*]

[1]Molecular Simulation Research Program,
Mexican Institute of Petroleum, Av. Lazaro Cardenas
No. 152, Col. San Bartolo Atepehuacan, cp 07730
Mexico D.F., Mexico
[2]Polymers Department, Materials Research Institute,
National University of Mexico,
Circuito Exterior S/N, Ciudad Universitaria, cp 04510
Mexico D.F., Mexico

ABSTRACT

A compositional flow model for predicting wax deposition in oil pipelines is presented. Sample calculations as a function of time have been obtained by a numerical solution to the two-dimensional heat and momentum equations, the laws of diffusion and a multisolid–wax thermodynamic model. Results show temperature, radial mass flux and wax deposition profiles as a function of time and position in the pipeline. Details of the numerical impementation of this model are described.

*Corresponding author. E-mail: clira@imp.mx

NOTATIONS

V_{max}	maximum axial velocity (m/s)
k	thermal conductivity of the mixture (W/m.K)
ρ_{ma}	average density of the mixture (Kg/m^3)
C_p	specific heat capacity of the mixture (J/Kg.K)
R_o	inner radius of the clean tube (m)
z	distance from pipe inlet (m)
T_o	tube inlet temperature (K)
T_a	constant ambient temperature (K)
T_r	reference temperature (K)
u	heat-transfer coefficient (W/m^2.K)
q_h	heat source (J/s.m^3)
D_m	diffusion constant (m^2/s)
ω	dimensionless weight function
C_1	parameter in diffusion constant model (N)
μ	viscosity (P.s)
w_i	weight fraction
ψ	L_s/L_x
α_t	coefficient of thermal expansion = $-(1/\rho_m)[\partial\rho_m/\partial T]$ (K^{-1})
ΔH_f	heat of fusion (J/mol)
L_x	number of moles in liquid phase per mol of mixture
L_s	number of moles in solid phase per mol of mixture
R	gas constant = 8.3143 (J/mol.K)
P	pressure (bar)
T	temperarture (K)
$\underline{Z}$	composition
J_i	mass flux of wax for component i (Kg/s.m^2)
t	time (h)
L	tube length (m)
Q	volumetric flow rate (m^3/s)
M	parameter in the power-law flow model
MW_i	molecular weight of component i (Kg/Kmol)
R_e	Reynolds number
R_w	time dependent inner radius of the tube (m)

INTRODUCTION

Deposition of solid organic materials in crude oil production systems is a major problem for the development of oil fields, since the deposition of waxes on the production wells can cause a serious economic loss due to the obstruction

of the fluid flow systems. For this reason, the development of predictive models for wax deposition in those fields is of significance. These models are intended to predict the deposition of wax out of solution on the pipe walls.

Most crude oils consist of various fractions of heavy hydrocarbons which are known to precipitate as paraffin deposits, due to either evaporation of volatile light ends (which otherwise act as naturally occurring solvents) or to drop in the system temperature. Accumulation of these solids in transport pipes and process equipment is an old and expensive problem in the petroleum industry. This problem is expected to increase in the future as existing reserves are being depleted and offshore explorations continue to grow.

The purpose of this study is to investigate the relevant mechanisms of wax deposition and to determine the expected composition and thickness of the deposits in the pipeline as a function of time and position. We used a novel approach based on a thermodynamic multisolid-phase model coupled to the transport conservation equations, and a compositional model for predicting the viscosity of the oil (1).

LITERATURE REVIEW

Most works on crude oil transport reported in the literature use empirical correlations to predict the pressure drop, liquid holdup temperature profiles, and other physical parameters (2,3). Burger et al. have investigated mechanisms of wax deposition, which occur as a result of lateral transport by diffusion, shear dispersion and Brownian diffusion (4). Fukui and Maeda carried out direct simulations of unsteady layer solidification for an eutectic binary fluid of lauric acid and myristic acid, which exhibits laminar flow between two parallel walls of different temperatures (5). Two-dimensional differential equations for momentum, heat, and mass transfer were solved using finite differences. The predictions were discussed with reference to the time-changes of the shape of the solid-liquid (S-L) interface, the growth rate, the concentration at the S-L interface, the super-cooled layer adjacent to the S-L interface, and the component concentration in the solid phase. More recently, Lindeloff (6) developed a pipeline deposition mechanism in which plug flow was assumed to simplify the problem. This profile is not affected by the thickness of the deposited wax layer. Another assumption in this model is that the viscosity of the fluid is independent of both temperature and concentration of wax components, which of course are not real in practical applications.

Furthermore, there are approaches which deal with the so-called particulate flowing systems; consisting of non-colloidally-sized fluid/solid systems, whose solid particles are already formed in the flow and interact between themselves with no aggregation forces (7). These pictures of liquid-solid flow do not capture the phenomena of wax deposition, in which the solids are solely formed at the cloud point of the solid-liquid equilibrium envelope and are transferred to the walls by

radial diffusion. In a pioneering work, Svendsen has presented a mathematical model of wax deposition in oil-pipeline systems which takes into account the mechanisms mentioned above (i.e., thermodynamic equilibrium and diffusion of the solid species) (8). In addition, the model takes into account the temperature profile along the pipe. This approach to the problem is used in the present work.

This work presents a numerical model for predicting wax deposition phenomena in crude oil pipelines. Sample calculations as a function of time for different initial and boundary conditions (i.e., flow rate, velocity profile, feed composition and well geometry), have been obtained by a numerical solution (based on the explicit form of the finite-difference forward method) to the two-dimensional heat equation, the laws of diffusion for multi-component mixtures, and thermodynamic-equilibrium expressions. The flow model described below is an extension of Svendsen's model in the sense that a multi-solid thermodynamic model with solid-liquid-vapor equilibrium is introduced (which will be described later in the paper), coupled with the equations of motion, energy and mass transfer. In the present work, results are presented for the simplified solid-liquid equilibrium approach.

THEORETICAL MODEL

System Description

The fluid consists of n hydrocarbon components. For multi-component systems, the composition and mole fraction of the phases are functions of pressure and temperature. Therefore, in a compositional three phase flow system (liquid-solid-vapor), the composition of the phases changes along the pipe (9).

Assumptions Related to Flow

Waxy oils are non-Newtonian fluids at temperatures below the WAP (wax appearance point), and Newtonian fluids otherwise (10). Since both viscosity and wax thickness may change along the pipeline, a turbulence contribution in the laminar sub-layer is possible, although it is assumed to be not significant. It is also assumed that the wax/oil boundary changes very slowly in the axial direction, so that a quasi-state model is applicable for all rate processes concerning energy and mass. Heat associated with frictional heating, axial thermal diffusion, and phase transitions is supposed to be negligible compared to heat convection.

The temperature distribution $T(r, z)$ is derived for a steady-state, laminar, non-Newtonian power-law flow with velocity profile $v_z(r)$:

$$v_z(r) = v_{\max}\left[1 - \left(\frac{r}{R_w}\right)^{m+1}\right] \tag{1}$$

If frictional heating and axial thermal diffusion can be ignored, the energy equation to be solved is:

$$v_z(r)\frac{\partial T}{\partial z} = \alpha\left(\frac{\partial^2 T}{\partial r^2} + \frac{1}{r}\frac{\partial T}{\partial r} + \frac{q_h}{k}\right) \tag{2}$$

where

$$\alpha = \frac{k}{\rho_{ma} C_p} \tag{3}$$

is the thermal diffusivity of the fluid with thermal conductivity k and specific heat capacity C_p, and q_h is a heat source term associated with a phase transition from the liquid to the solid state. The boundary conditions are:

$$T(r, 0) = To \qquad 0 \le r \le R_o \tag{4.1}$$

$$T(0, z) = \text{ finite } z > 0 \tag{4.2}$$

$$T(R_o, z) = T_\alpha(z) \tag{4.3}$$

$$\frac{\partial T}{\partial r} = -\frac{u}{k}[T(R_o, z) - T_\alpha(z)] \tag{4.4}$$

Equation (4.4) describes the interfacial heat transfer from the pipe inner wall to the liquid. $T_\alpha(z)$ is the geothermic temperature profile along the pipe. Negligible resistance to heat conduction is assumed across the pipe wall.

Using forward finite differences, the solution of Equation (2) for the plug flow case (i.e., $m \to \infty$ in Equation (1)), and with $q_h = 0$, is written in dimensionless form as:

$$\frac{\partial \theta}{\partial \phi} = \left(\frac{\partial^2 \theta}{\partial \gamma^2} + \frac{1}{\gamma}\frac{\partial \theta}{\partial \gamma}\right) \tag{5}$$

where:

$$\theta = \frac{T - T_o}{q_1(z)\dfrac{R}{k}} \qquad \gamma = \frac{r}{R} \qquad \phi = \frac{zk}{\rho C_p v_{\max} R^2}$$

The forward finite difference formulation of the above equations is defined:

$$\begin{aligned} \frac{\partial \theta}{\partial \phi} &= \frac{\theta_{i,j+1} - \theta_{i,j}}{\Delta \phi} \\ \frac{\partial \theta}{\partial \gamma} &= \frac{\theta_{i+1,j} - \theta_{i,j}}{\Delta \gamma} \\ \frac{\partial^2 \theta}{\partial \gamma^2} &= \frac{\theta_{i+1,j} - 2\theta_{i,j} + \theta_{i-1,j}}{(\Delta \gamma)^2}. \end{aligned} \tag{6}$$

Substituting Equation (6) into Equation (5) gives:

$$\theta_{i,j+1} = \theta_{i,j} + \lambda\left[\theta_{i+1,j}\left(1+\frac{1}{i}\right) - \theta_{i,j}\left(2+\frac{1}{i}\right) + \theta_{i-1,j}\right] \tag{7}$$

where

$$\lambda = \frac{\Delta\phi}{(\Delta\gamma)^2} \tag{8}$$

with the following boundary conditions:

$$\phi = 0 \quad \theta = 0 \tag{9.1}$$

$$\gamma = 0 \quad \theta = \text{finite} \tag{9.2}$$

$$\gamma = 1 \quad \frac{\partial\theta}{\partial\gamma} = -1 \tag{9.3}$$

Furthermore, it is assumed that the radial mass flux can be expressed by the following form of Fick's law:

$$J = \sum_i J_i = -\Gamma_m \rho_m \left[\sum_i \omega_i\right] \frac{1}{T}\frac{\partial T}{\partial r} = -\Gamma_m \rho_m \omega \frac{1}{T}\frac{\partial T}{\partial r} \tag{10}$$

where the average diffusion constant is defined in a similar empirical form than the one used by Svendsen, i.e.:

$$\Gamma_m = \frac{C_1}{\mu} \tag{11}$$

The dimensionless function $\omega = \sigma - \varepsilon$ is expressed as:

$$\varepsilon_i = \frac{w_i T \alpha_t}{1 + \psi K_i} \tag{12a}$$

$$\sigma_i = \frac{w_i\left[T(1+\psi)^2 \frac{\partial Lx}{\partial T} + \psi \frac{\Delta H_{fi}}{RT}\right] K_i}{(1+\psi K_i)^2} \tag{12b}$$

where the K_i are the equilibrium constants which determine the solid-liquid-vapor equilibrium of the mixture. The thermodynamics of this problem are obtained from the multisolid approach of Lira-Galeana et al. (11). At a given temperature level, the total precipitated wax is given by the sum of the contributions of all solid phases that exist in equilibrium at that temperature. Lira-Galeana et al. established that the components that precipitate are those which satisfy the following test of thermodynamic stability

$$f_i(P,T,z) - f^{\text{pure}}{}_i(P,T) \geq 0 \quad (i = 1, 2, \ldots, N) \tag{13}$$

Further details on the use of the above equilibrium approach can be found elsewhere (12,13; Won, 1986).

According to Svendsen, the calculation of deposition and wax thickness is given by:

$$M_w(t,z) = \sum_i M_{wi}(t,z) = \sum_i 2\pi \int_0^t \int_0^z R_w J_i \, dz \, dt \tag{14}$$

where $M_w(z,t)$ is the total amount of deposition at time t at a given distance from the inlet ($z = 0$ to $z = z_o$). The increase in amount of deposition per unit length of pipeline at time t. It is possible to express $\partial Mw/\partial z$ at time t as:

$$\frac{\partial M_w}{\partial z} = \sum_i \frac{\partial M_{wi}}{\partial z} = \sum_i 2\pi \int_0^t R_w J_i \, dt \tag{15}$$

$$\frac{\partial M_w}{\partial z} = \pi\left(R_o^2 - R_w^2\right)\rho_{wa} \tag{16}$$

The solid wax deposition is somewhat compressed, so $\rho_w > \rho_m$. Solving the latter equation for R_w, one obtains:

$$R_w = \left(R_0^2 - \frac{1}{\pi\rho_w}\frac{\partial M_w}{\partial z}\right)^{\frac{1}{2}} \tag{17}$$

The corresponding wax thickness $h(z,t)$ is calculated from: $h = R_o - R_w$. The total deposition rate is:

$$\frac{dM_w}{dt} = \sum_i \frac{dM_{wi}}{dt} = \sum_i 2\pi \int_0^L R_w J_i \, dz \tag{18}$$

In this work, the approach used by Werner et al. (1998) for the calculation of petroleum fluids viscosities is employed, i.e.:

$$\mu(P,T) = \left(\frac{D+P}{D+P_o}\right)\mu(P_o,T)\exp\left[\alpha\left(\frac{1}{T} - \frac{1}{T_o}\right)\right] \tag{19}$$

where α is a function of $z_o = \ln[\mu(P_o, T_o)]$ ($P_o = 1$ bar; $T_o = 298$ K), while D is a parameter which is a function of the viscosity at the current temperature of the mixture, $\mu(P_o, T)$:

$$D[MPa] = \exp(-0.192z) \tag{20}$$

and $z = \ln\mu(P_o, T)$.

It is necessary to point out that this approach is valid for small deposited-layer thickness, since no consideration is given to the change in the heat transfer coefficient as the layer increases.

RESULTS

Let us consider a model system with two representative crude oil components of different molecular weight, with realistic values of well geometry and flow rate. These are given in Table 1.

The calculation is performed from the bottom of the well up to the surface. Given a geothermic axial temperature profile, the heat flow is transferred across the pipe wall, so that the liquid temperature diminishes along the pipe from bottom to surface conditions. Starting from To and Po (temperature and pressure at the bottom of the reservoir), an initial guess of the pressure is used at each grid point (the pressure gradient may be assumed linear). According to the flow diagram, a local mass balance is required to check the assumed pressure. The pressure value is updated to calculate the following temperature profile. The following flowchart shows how the calculations are carried out throughout the geometry (Fig. 1).

In Figure 2, the axial temperature profile of the bulk fluid and the geothermic temperature gradient at the wall pipe, taken from field data from a typical well located in South Mexico, are shown. Past an initial rapid growth of approximately 333 K during the first 500 m, the temperature profile of the bulk fluid is linear up to around 4,000 m. Temperature of the fluid increases from 318 K at the inlet to 403 K at the bottom conditions. Notice that differences between the fluid temperature and the temperature at the wall increase for depths higher than 1000 m. These boundary conditions are considered in the calculations shown below.

Table 1. Model Parameters and Input Information

Model Parameters (Units)	Values
Pipe radius, R_o (m)	0.15
Pipe length, L (m)	3860.0
Volumetric flow rate, Q (m^3/h)	500
Molecular weight, PM_1 (Kg/Kmol)	222
Molecular weight, PM_2 (Kg/Kmol)	580
Tube inlet temperature T_o (K)	434
Reynolds number, R_e	57970

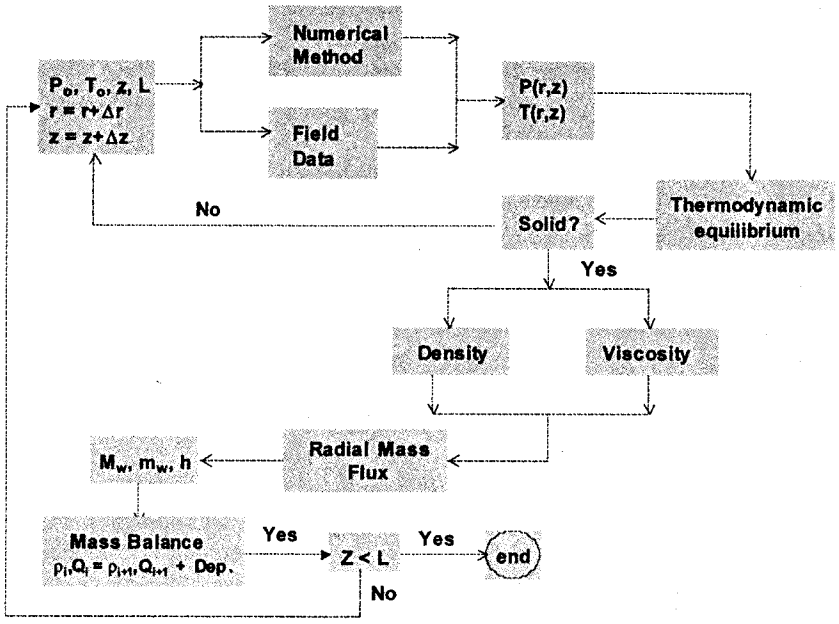

Figure 1. Calculation procedure.

Figure 3 shows the radial temperature profile of the fluid and the temperature gradient calculated at the mid-depth of the well. This profile is obtained straightforwardly from the finite difference solution of Equation (7) with boundary and initial conditions (9). Here plug flow is considered, and the temperature

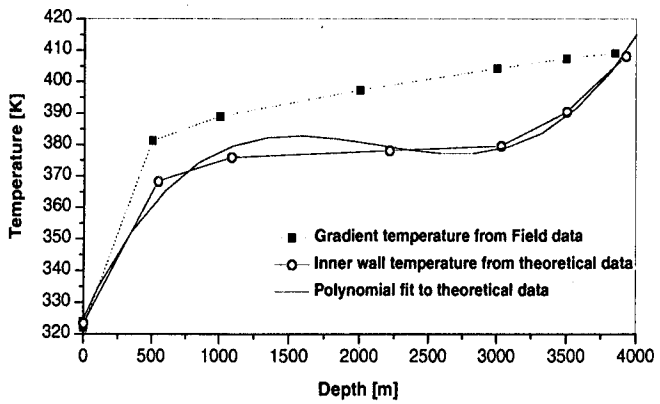

Figure 2. Temperature versus well depth for a typical south Mexican well.

of the pipe wall in contact with the liquid is assumed to vary in the axial direction according to the geothermic gradient shown in Figure 2. The interfacial heat transfer coefficient is constant for a Newtonian, laminar flow in a pipe. From the axial and radial temperature profiles, the thermodynamic equilibrium calculations are implemented at each grid point.

Figure 4 depicts the experimentally measured pressure profile along the well from field data. Pressure increases almost linearly from around 138 bar at the inlet conditions up to approximately 413 bar at the bottom of the well. These pressure values are considered in the calculation of the thermodynamic equilibrium at each axial grid point, since no radial variation of the pressure is taken into account.

The total radial mass flux and that of the components of the precipitated solid phase are shown in Figure 5. The wall is located at 0.15 m. J_1 is the mass flux of the light component (molecular weight = 222) and J_2 is that of the heavy component (molecular weight = 580). Note that the magnitude of the flux of the heavy component is almost twice that of the light component.

The radial mass flux increases substantially in regions close to the wall, simultaneously to the change in the gradient temperature profile (Fig. 2). This is expected, since according to Equation (10), the temperature and temperature gradient provide the driving force for radial diffusion flux.

It is possible to obtain the mass per unit volume of wax deposited on the pipe wall using Equation (15). Results are plotted in Figure 6, where the mass

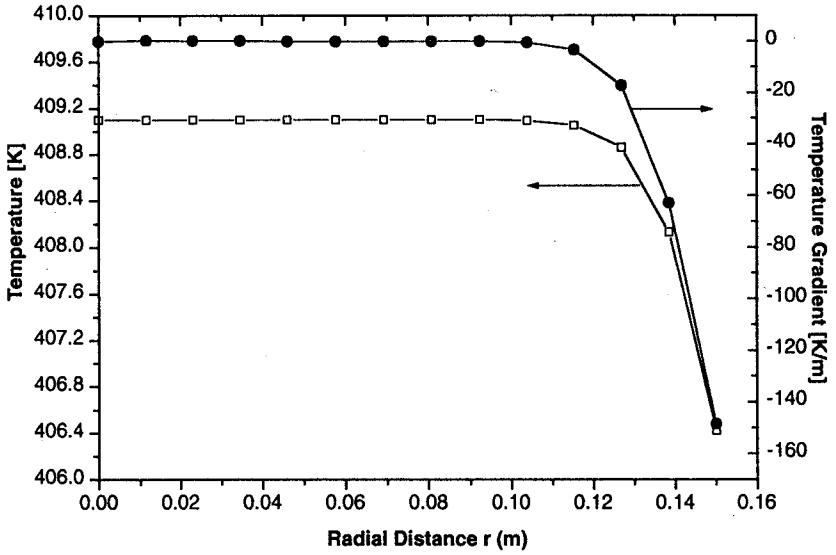

Figure 3. Fluid temperature and gradient as a function of radial distance at $z = 1895$ m.

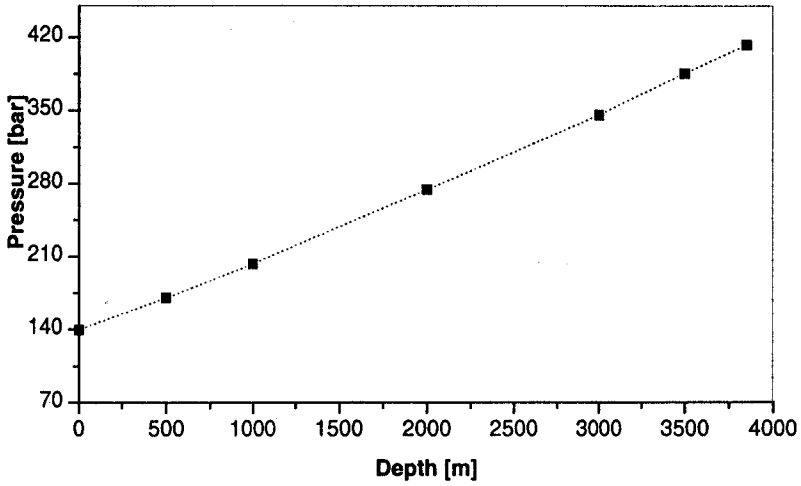

Figure 4. Pressure gradient for a typical south Mexican well.

deposited is given as a function of time for a fixed well depth (1895 m). As shown, the amount of heavy component dominates and the deposition rate (slope of the curves in Fig. 6) increases for larger times. Past 80 h, the deposited amount profile of components 1 and 2 in the mixture with distance from the inlet is plotted in Figure 7. The wax deposition amount of the heavy component increases for larger distances from the inlet at very high depths. Also, the thickness of the deposited

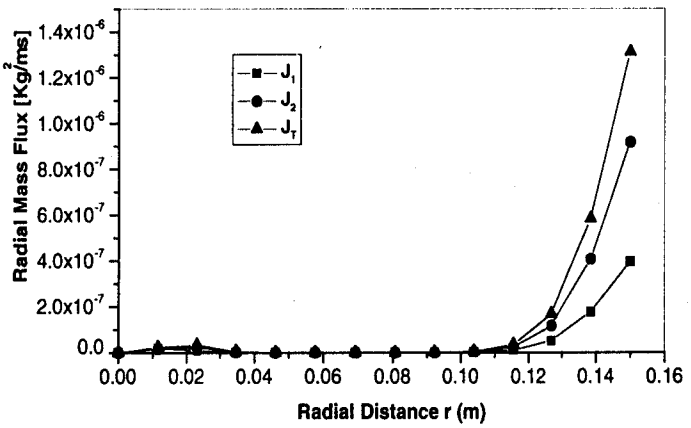

Figure 5. Radial mass flux for each component in the mixture at $z = 1895$ m.

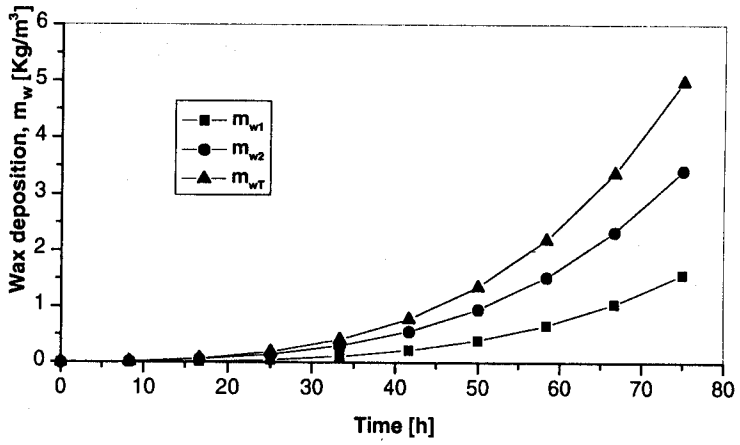

Figure 6. Deposition of each component at $z = 1895$ m as a function of time.

layer, calculated from Equation (17), is plotted with the well depth in Figure 8 for various times. Observe that an abrupt increase in the wall thickness occurs at 1000–1500 m from inlet. This is also noticeable in Figure 7 for the heavy component. The sudden increase in the wall thickness is partly due to the increase in temperature difference between the temperature of the well's wall and that of the liquid.

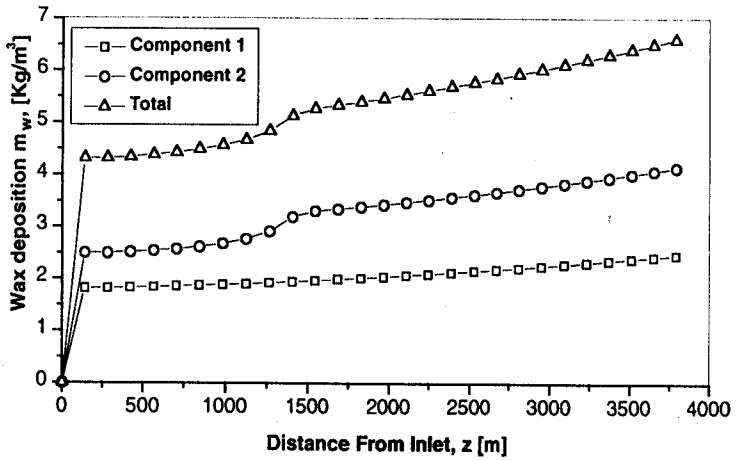

Figure 7. Deposition of each component after 80 hr of calculation as a function of position.

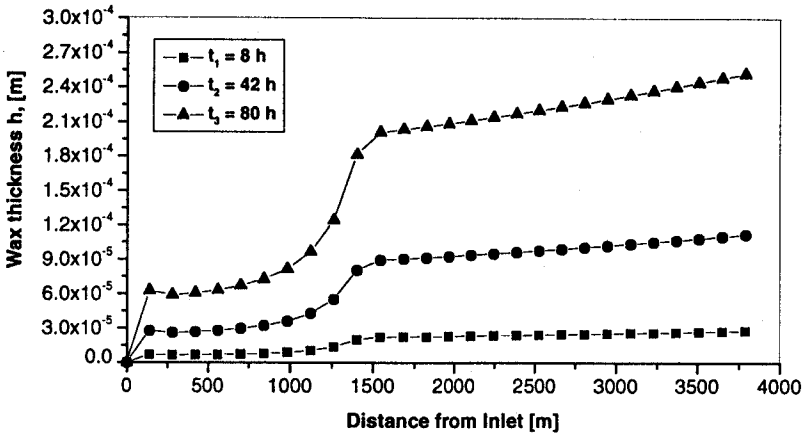

Figure 8. Thickness layer distribution as a function of time.

CONCLUSIONS

Wax deposition has been predicted by a model based on Svendsen's approach for a two component mixture in liquid-solid equilibrium undergoing plug flow (8). Experimental field data of the fluid temperature and pressure along the length of a typical inshore well, and geothermic data are considered in the radial diffusion calculations. Results show that the deposited layer contains a larger amount of the heavier component. This is predicted as a function of time and distance from the inlet. An extension to incorporate a non-Newtonian velocity profile with a three-phase multi-component mixture is currently under consideration.

REFERENCES

1. Werner, A.; De Hemptinne, J.C.; Behar, F.; Behar, E.; C. Boned. A New Viscosity Model for Petroleum Fluids with High Asphaltenes Content. Fluid Phase Equilibria, Vol. 147, 1998; 319–341.
2. Ansari, A.M.; Sylvester, N.D.; Sarica, O.; Shoham, O.; Brill, J.P. A Comprehensive Mechanistic Model for Upward Two-Phase Flow in Wellbore, SPE Production & Facilities, May 1994; 143–152.
3. Brill, J.P.; Arirachakaran, S.J. State of Art in Multiphase Flow. JPT. May 1992; 538–541.
4. Burger, E.D.; Perkins, T.K.; Striegler J.H. Studies of Wax Deposition in the Trans Alaska Pipeline. J. Petro. Technol. **1981**, 1075–1086.
5. Fukui, K.; Maeda, K. Numerical Simulation of Dynamic Layer Solidification

for a Eutectic Binary System. J. of Chem. Eng. of Japan **1998**, *31* (2), 445–450.
6. Lindeloff, N. *Formation of Solid Phases in Hydrocarbon Mixtures*, PhD. Thesis; Department of Chemical Engineering, Technical University of Denmark, 1999; Ch. II, 4–6.
7. Johansen, S.T. The Deposition of Particles on Vertical Walls. J. Multiphase Flow **1991**, *17* (3), 355–376.
8. Svendsen, J.A. Mathematical Modeling of Wax Deposition in Oil Pipeline Systems. AIChE J. **1993**, *39* (8), 1377–1388.
9. Goyon, J.C.; Shoham, O.; Brill, J.P. Analysis of Computational Procedures for Multicomponent Flow in Pipelines. SPE. **1988**, *17573*, 219–232.
10. Wardhaugh, L.T.; Borger, D.V. Flow Characterization of Waxy Crude Oils: Application to Pipeline Design. AIChE J. **1991**, *37* (6), 871.
11. Lira-Galeana, C.; Firoozabadi, A.; Prausnitz, J.M. Thermodynamics of Wax Precipitation in Petroleum Mixtures. AIChE J. **1996**, *42* (1), 239.
12. Peng, D.Y.; Robinson, D.B. A New Two- Constant Equation of State. Ind. Eng. Chem. Fund. **1976**, *15* (59).
13. Won, K.W. Thermodynamic Calculation of Cloud Point Temperatures and Wax Phase Compositions of Refined Hydrocarbon Mixtures, Fluid Phase Equilibria, Vol. 53, 1989; 377.

Received December 7, 1999
Accepted February 15, 2000